Carbohydrate Polymers 105 (2014) 270–275

Contents lists available at ScienceDirect

Carbohydrate Polymers

journal homepage: www.elsevier.com/locate/carbpol

# Synthesis of poly(2-(2-methoxyethoxy)ethyl methacrylate) hydrogel using starch-based nanosphere cross-linkers

Chang Liu[a,b], Ying Tan[a,*], Kun Xu[a], Yangling Li[a,b], Cuige Lu[a,b], Pixin Wang[a,*]

[a] Key Laboratory of Polymer Ecomaterials, Changchun Institute of Applied Chemistry, Chinese Academy of Science, 130022, PR China
[b] Graduate University of Chinese Academy of Sciences, Beijing 100049, PR China

ARTICLE INFO

*Article history:*
Received 13 November 2013
Received in revised form 20 January 2014
Accepted 22 January 2014
Available online 31 January 2014

*Keywords:*
Hydrogel
Thermosensitive
Starch-based nanosphere
LCST gap
Mechanical strength

ABSTRACT

Biodegradable thermosensitive hydrogels have attracted great interest because of their potential in biomedical applications. Herein, we present a novel, thermoresponsive poly(2-(2-methoxyethoxy)ethyl methacrylate) hydrogels with starch-based nanospheres as cross-linkers (NMH). NMHs exhibit a narrow lower critical phase transition temperature (LCST) range and high mechanical strength compared with conventional, small molecular cross-linked hydrogels (CMH). Fourier transform infrared (FT-IR) spectroscopy confirms that the NMHs are degradable in aqueous medium. The phase transition temperature of the NMHs is ~4 °C compared with ~25 °C for CMH. The NMHs can sustain strength of 12.2 MPa, 10 times more than that of CMH. Moreover, the deswelling rate of NMHs is faster than CMH. The different concentrations of nanospheres can efficiently regulate the various properties of NMHs. The NMHs have excellent properties because of its even network structure formed by nanosphere cross-linkers.


## 1. Introduction

Intelligent hydrogels are interesting because they can swell or deswell in response to various external stimuli, such as temperature (Gates, Park, & Xia, 2000; Hu & Huang, 2003), salts (Xu et al., 2010), pH (Lee & Braun, 2003), and electric field (Kwon, Bae, & Kim, 1991; Matsubara, Watanabe, & Takeoka, 2007; Sharma et al., 2004). These environmentally sensitive properties endow intelligent hydrogels a very wide application prospect in tissue engineering, pharmaceutical systems, medical treatment, artificial organs, physiology, and environmental protection (Chang, van Spreeuwel, Zhang, & Varghese, 2010; Liu, Liu, Chen, & Liu, 2008). Polyoligo(ethyleneglycol) methylether methacrylate (POEGMA) is a thermoresponsive polymer that consists of a hydrophobic hydrocarbon main chain with numerous hydrophilic oligo(ethylene glycol) side chains. Unlike the typical temperature-responsive polymer poly(*N*-isopropylacrylamide) (PNIPAM), which has a lower critical phase transition temperature (LCST) of 32 °C, POEGMA shows excellent in vitro or in vivo biocompatibility (Gao et al., 2009; Lutz, Akdemir, & Hoth, 2006; Lutz, Weichenhan, Akdemir, & Hoth, 2007). Additionally, the LCST of POEGMA can be tuned by using the length of the oligo(ethyleneglycol) side chains from 23 to 90 °C without introducing co-monomers of different chemical properties (Lutz & Hoth, 2006).

Hydrogel as a stimulus response material should have fast response to the external stimulus, especially in applications that demand an on-off behavior, for instance drug delivery (Luo, Kirker, & Prestwich, 2000) and enzyme immobilization (Hoshino, Taniguchi, Katagiri, & Fujii, 1992). However, POEGMA hydrogels synthesized conventionally (organic small molecular cross-linker) showed a continuous variation of transmittance in a wide range of temperature, apart from having poor mechanical properties. These defects could be considered as obstacles for the use of POEGMA hydrogels as core materials. Recently, many efforts have been made for increasing the response rate of thermosensitive hydrogels. In order to overcome the diffusion limit in aqueous medium, porous hydrogels have been prepared by heterogeneous polymerization at temperatures above the LCST (Gotoh et al., 1998; Iizawa et al., 2007; Iizawa et al., 2012; Zhang & Zhuo, 2001), in the presence of surfactants (Antonietti, Caruso, Göltner, & Weissenberger, 1999), or by incorporating silica particles (Serizawa, Wakita, & Akashi, 2002) followed by extraction. Another approach to increase the response rate is creating a hydrogel with homogeneous, nanoscale-cross-linked network, for instance from clay. Such a material exhibits a fast stimulus response because of the isotropic nature of the network, where clay nanosheets are evenly dispersed (Haraguchi, Farnworth, Ohbayashi, & Takehisa, 2003; Haraguchi & Takehisa, 2002). Furthermore, introducing nanoscale components into the hydrogel increases the mechanical strength because the filler nanoparticles interact with the polymer chain matrix, causing stiff confinement of the chains and retardation of their orientational dynamics (Sharma et al., 2004).

* Corresponding author. Tel. +86 431 85262629; fax: +86 431 85262629.
*E-mail addresses:* tanying@ciac.ac.cn (Y. Tan), pxwang@ciac.ac.cn (P. Wang).

0144-8617/$ – see front matter © 2014 Elsevier Ltd. All rights reserved.
http://dx.doi.org/10.1016/j.carbpol.2014.01.078

We have recently shown that starch-based nanosphere cross-linkers can efficiently improve the mechanical strength of polyacrylamide (Tan et al., 2009) and PNIPAM hydrogels (Tan et al., 2010). Herein, we extend this approach to novel poly(2-(2-methoxyethoxy)ethyl methacrylate) (NMH) hydrogels that exhibit a fast response rate in a narrow LCST range and an increased mechanical strength as well as a fast response rate. Importantly, the biodegradable cross-linking nanoparticles facilitate its biomedical applications. In addition, the effects of the cross-linking density on the swelling and deswelling properties of hydrogels have been investigated in detail.

## 2. Experiment

### 2.1. Materials

The corn starch was purchased from Changchun Dacheng Corn Development Co., Ltd. (China). The amylose and amylopectin content is 27% and 73%, respectively (Juliano et al., 1981). Acetated allylic starch (AAS) was synthesized according to a previous method (Tan et al., 2009). The macromolecular weight (Mw) of AAS is $1.8 \times 10^5\,g\,mol^{-1}$ according to GPC characterization (Narumi et al., 2006). The degree of substitution (DS) of the acetate and allylic groups is 2.1 and 0.19, respectively. 2-(2-Methoxyethoxy)ethyl methacrylate ($MEO_2MA$) and diethyleneglycol dimethacrylate (DEGMA) were purchased from Sigma. 2,2-Dimethoxy-2-phenylacetophenone was purchased from TCI. All the other chemicals were analytical reagent grade and used without further treatment.

### 2.2. Preparation of AAS nanospheres

AAS (0.5 g) was dissolved in acetone (50 mL), distilled water (50 mL) was then added dropwise to the AAS solution with stirring at 100 rpm. The resulting nanosphere suspension was stirred at room temperature until the acetone completely vaporized from the solution.

### 2.3. Preparation of $PMEO_2MA$ hydrogels

AAS nanosphere aqueous solution (5 wt%; 1.4 mL) and 2,2-dimethoxy-2-phenylacetophenone ethanol solution (10 wt%; 0.7 mL) were added into a test tube charged with $MEO_2MA$ (3.5 g), ethanol (1.9 mL), and distilled water (2.5 mL) under sonication. The mixture was deaerated ($N_2$ stream) for 10 min, and photopolymerized under UV light (365 nm; Philips, PL-L, 36 W) for 15 h at ambient temperature.

### 2.4. Preparation of conventional $PMEO_2MA$ hydrogel

2,2-Dimethoxy-2-phenylacetophenone ethanol solution (10 wt%; 0.7 mL) was added to a test tube charged with $MEO_2MA$ (3.5 g), DEGMA (8.3 mg), ethanol (1.9 mL), and distilled water (1.4 mL). The mixture was deaerated ($N_2$ stream) for 10 min, and photopolymerized under UV light (365 nm; Philips, PL-L, 36 W) for 15 h at ambient temperature.

### 2.5. NMR characterization

AAS was dissolved in DMSO-$d_6$ at 25 °C and NMH3 hydrogel were swelled in $CDCl_3$. The $^1H$ NMR spectra (400 MHz) were recorded on a Bruker AV400 spectrometer (Ettlingen, Germany) at the same temperature.

### 2.6. Scanning electron microscopy (SEM)

The microapperance of the AAS nanospheres and hydrogels were characterized on XL 30 ESEM (Philips). The as-synthesized sample was added dropwise onto a silicon plate, which was sputter-coated with a thin layer of gold prior to the SEM analyses, and dried in air. The synthesized hydrogel (CMH and NMH3) was freeze-dried and covered with gold before measurement.

### 2.7. Double bond content in AAS

The double-bond content in the AAS nanospheres was calculated as follows:

$$M_{AAS} = 162 + (M_{allyl} - 1) \times DS_{allyl} + (M_{acetyl} - 1) \times DS_{acetyl} \quad (1)$$

$$n_{allyl} = \frac{m_{AAS}}{M_{AAS} \times DS_{allyl}} \quad (2)$$

where 162 corresponds to the molecular mass of a glucose unit; $M_{AAS}$, $M_{allyl}$, and $M_{acetyl}$ represent the molecular weights of AAS, allyl, and acetyl, respectively; $DS_{allyl}$ and $DS_{acetyl}$ represent the degree of substitution of allyl and acetyl, respectively; $n_{allyl}$ represents the moles of allyl, which equals that of the double bonds; and $m_{AAS}$ represented the mass of dry AAS in the hydrogels. Because the allyl groups are mainly located at the periphery of the nanospheres (Tan et al., 2009), we deem that the content of double bonds in AAS is approximately equal to that of in AAS nanospheres (Tasaki, 1996).

### 2.8. Infrared spectroscopy

The FT-IR spectra of NMH5 hydrogel fragments incubated in phosphate buffered solution (PBS; pH 7.4) at selected degradation time points at 20 °C were recorded on Thermo Nicolet Avetar 370 (Pike Technologies, Madison, WI) attenuated total reflection fourier transform-infrared spectroscope (ATR-FTIR) in the range 4000–500 $cm^{-1}$.

### 2.9. Equilibrium swelling ratio of hydrogels

Dried hydrogel disks were allowed to swell in distilled water at 18 °C and weighed after gently drying the surface with filter paper. The disks were weighed daily to constant weight, which indicates that swelling equilibrium has been reached. The ratio of the weight in equilibrium swelling state to the dry weight (swelling ratio) was calculated.

### 2.10. Mechanical strength measurements

The mechanical properties of cylindrical hydrogel samples (diameter of 14 mm, thickness of ~14 mm) were measured on an INSTRON-1121 testing machine at room temperature. The crosshead speed was 2 mm $min^{-1}$. The strength ($\delta$) was calculated as follows:

$$\delta = \frac{\text{Load}}{3.14r^2} \quad (3)$$

where $r$ is the initial unload radius. The strain to failure under compression is calculated as the thickness of the compressed hydrogel relative to the initial thickness.

### 2.11. Deswelling properties

Disk-shaped samples (diameter of 8 mm, thickness of 5 mm) were preequilibrated at 5 °C to constant weight, and then abruptly submerged in water heated to 30 °C. The disks were removed at predetermined times and the weight recorded until an equilibrium

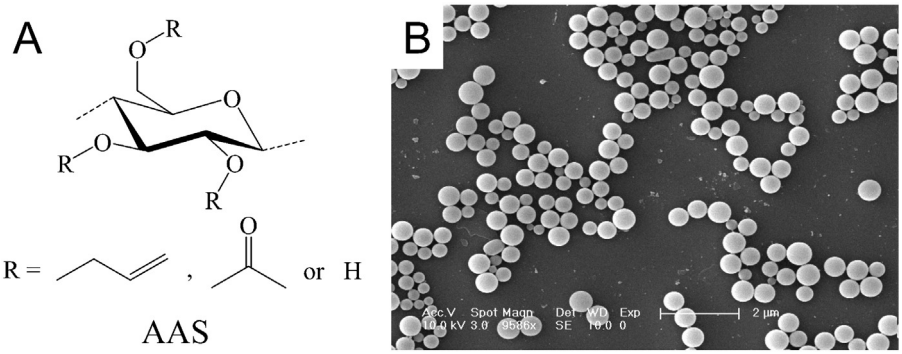


**Fig. 1.** Potential macromolecular structure of AAS (A) and the SEM image of starch-based nanospheres formed by nano-coprecipitation (B).

was reached. $Q_n/Q_0$ was plotted as a function of time, where $Q_n$ denotes the swelling ratio of a polymer at each record time and $Q_0$ denotes the equilibrium swelling ratio at 5 °C.

### 2.12. Lower critical phase transition temperature

The transmittance of hydrogel specimens (dimensions 20 mm × 10 mm × 1 mm) at 550 nm in deionized water was monitored on a UV–vis spectrophotometer as a function of temperature at a heating rate of 2 °C $min^{-1}$. The temperature at 50% transmittance was taken as the LCST.

## 3. Results and discussion

### 3.1. Preparation of AAS nanospheres

AAS (Fig. 1A) was synthesized according to a published method (Tan et al., 2009). The degree of substitution (DS) of the acetate and allylic groups determined by $^1$H NMR is 2.1 and 0.19, respectively. The $^1$H NMR spectra of the sample were illustrated in Fig. 2A. The nanospheres were fabricated by nanoprecipitation at the acetone/water interface. After the complete removal of acetone, spherical AAS nanoparticles with diameter ~300 nm were obtained (Fig. 1B). The AAS nanoparticles were used as the nanoscale cross-linker to form $MEO_2MA$ hydrogels via UV-initiated free-radical polymerization.

### 3.2. Hydrogel synthesis

The AAS nanosphere cross-linkers were used for the synthesis of $PMEO_2MA$ hydrogels by UV-initiated free-radical polymerization. Two factors are crucial during the polymerized process. First, ethanol is added to maintain complete dissolution of the $MEO_2MA$ monomer. Second, the addition of a nanoparticle aqueous solution should be conducted under sonication to ensure that the nanospheres are well dispersed. The hydrogels swell but do not dissolve in water, demonstrating that nanospheres successfully cross-linked $MEO_2MA$ monomers during the reaction. Moreover, According to the $^1$H NMR characterization in Fig. 2B, the signal in 5.8–5.9 ppm is disappeared in the NMH3, which is the carbon-carbon double bond of AAS. It is suggested that the allyl groups of AAS nanospheres participated the polymerized process.

The swelling characteristics are one of the most critical factors for hydrogels. The equilibrium swelling ratios of CMH and NMHs with defferent AAS nanospheres content is shown in Table 1. All hydrogels readily swell in water and reach equilibrium in 2 d. The equilibrium swelling ratios slightly increased from 10.5 (w/w) to 12.9 (w/w) when the nanosphere concentration was increased from 0.2 to 2.0 wt%, presumably because starch-based nanospheres with some of hydrophilic groups can absorb a certain amount of water, so that the swelling ratios increase with the increasing of nanospheres content in NMHs. Notably, when the contents of nanoparticle increased continuously from 2.0 wt% to 4.0 wt%, the equilibrium swelling ratios decreased from 12.9 to 7.4. This is because the gradually increasing cross-linking density squeezes the cyberspace containing water despite the effect of water absorb ability of AAS has already existed. Even though CMH and NMH5 have the same amount of double bonds, the equilibrium swelling ratio of CMH is 7.2 (w/w), smaller than that of NMH5 which is 11.8 (w/w).

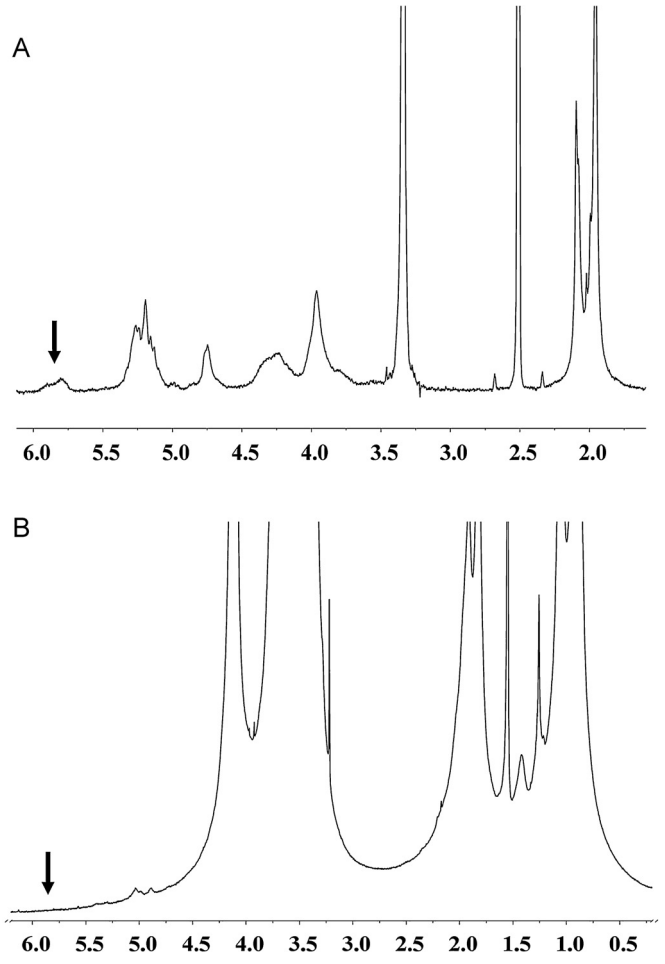


**Fig. 2.** $^1$H NMR spectrum of AAS (A) and NMH3 hydrogel (B).

**Table 1**
Effects of nanosphere concentration on properties of poly($MEO_2MA$) hydrogels[a]. Effects of nanosphere concentration on properties of CMH and NMHs.

| Hydrogel | AAS nanospheres in monomer (wt%) | LCST (°C) | Phase transition gap (°C) | Strength (MPa) | Strain to failure | Equilibrium swelling ratio |
|---|---|---|---|---|---|---|
| CMH[b] | 0 | 20.5 | 25 | 1.2 ± 0.33 | 90.5 ± 1.3% | 7.2 ± 0.6 |
| NMH1 | 0.2 | 22.2 | 15 | 5.6 ± 0.86 | 99.2 ± 0.9% | 10.6 ± 0.8 |
| NMH2 | 0.5 | 22.5 | 13 | 7.3 ± 0.52 | 98.3 ± 0.7% | 10.8 ± 0.5 |
| NMH3 | 1.0 | 22.7 | 7 | 9.3 ± 0.75 | 98.6 ± 0.6% | 11.4 ± 0.4 |
| NMH4 | 2.0 | 23.0 | 6 | 10.6 ± 0.42 | 97.4 ± 0.8% | 12.9 ± 0.6 |
| NMH5 | 3.0 | 23.2 | 5 | 12.2 ± 0.82 | 95.2 ± 1.0% | 11.8 ± 1.1 |
| NMH6 | 4.0 | 23.4 | 4 | 15.6 ± 0.56 | 94.0 ± 1.1% | 7.4 ± 0.9 |

[a] The monomer concentration is 35 wt%, the volume ratio of ethanol/water is 40/60 v/v.
[b] Conventional corss-linking agent DEGMA was used, with concentration 1.8 mmol/mol $MEO_2MA$.

### 3.3. Phase transition properties

Polymers containing short oligo(ethyleneglycol) side chains exhibit thermoresponsive properties in water because of the balance between the hydrophilic and hydrophobic moieties in the polymer. The ether oxygen atoms form stabilizing H-bonds with water molecules (Israelachvili, 1997; Tasaki, 1996), whereas the nonpolar hydrocarbon backbone exert a competitive hydrophobic effect (Lutz , Andrieu , Üzgün , Rudolph , Agarwal, 2007; Maeda, Kubota, Yamauchi, Nakaji, & Kitano, 2007). The increasing temperature weakens the hydrogen bonds, at the same time, strengthens the interaction between the hydrophobic backbones. For the reasons given above, the polymers shrink, and turn opaque. The loss of transmittance can be used to monitor the phase transition process; the temperature of 50% transmittance was taken as the LCST. Table 1 and Fig. 3 show the LCSTs of CMH and NMHs in aqueous medium when the temperature was varied from 5 to 32 °C. The transmittance of CMH decreases gradually, without abrupt transitions, throughout the entire testing temperature range. The LCST of CMH is 20.5 °C. For NMHs, the corresponding LCSTs move to higher temperatures (from 22.2 to 23.4 °C) with increase in the nanosphere concentration. This elevation of LCST is most likely due to the presence of a large amount of hydroxy groups in the starch-derived nanoparticles, they can form hydrogen bonds with the surrounding water. Moreover, the range of temperatures with transmittance gradients (LCST gap) is narrow for the nanosphere-cross-linked NMHs. The LCST gaps change from 15 to 4 °C when the nanosphere content increases from 0.2 to 4.0 wt%, that is, more nanoparticles result in sharper phase transitions. Conventional organic small molecule cross-linkers lead to significantly large thermal fluctuations in the gels (such as CMH) because of the heterogeneous aggregation of cross-linking points (Bastide & Leibler, 1988; Shibayama, 1998). Hence, when the temperature increase, some regions in the CMH shrink first, blocking the path of light through the corresponding parts of the sample, even though the temperature is far below the LCST. This explains the shallow transmittance gradient for this hydrogel. In contrast, AAS nanoparticles are well distributed in the hydrogel and construct more homogeneous networks. Thus, the transmittance gap becomes narrower in the presence of nanospheres cross-linker because of the contraction (shrinkage) of NMHs becoming more synchronous with the temperature increase.

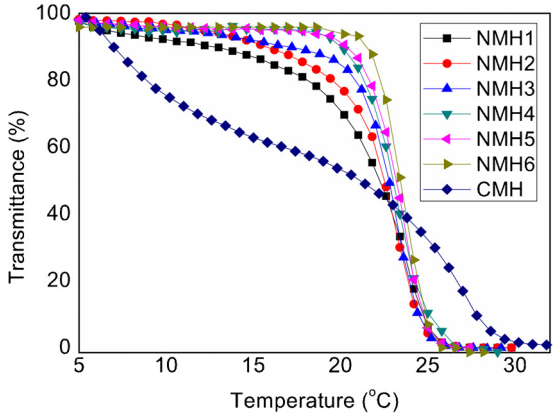


**Fig. 3.** Plots of transmittance at 550 nm as a function of temperature (heating rate of 2 °C $min^{-1}$) for CMH and NMHs in water.

### 3.4. Mechanical properties

The mechanical strength of hydrogels is very important for practical applications that require facing external forces. The compression stress–strain curves of the hydrogels with DEGMA (CMH) and nanosphere (NMHs) cross-linkers are compared in Fig. 4A. Significantly, the NMH5 hydrogel sustains strength of 12.2 MPa, 10 times more than that of CMH (1.2 MPa). The strain to failure of CMH is 90.5%, the value of NMHs is higher from 99.2% to 94.0%. The strain to failure in general is failing as the AAS nanospheres added from 0.2 wt% to 4.0 wt%.

Generally, the mechanical properties of hydrogel is determined by its microstructure. As shown in Fig. 5, the conventional hydrogel cross-linked by DEGMA (CMH) exhibited a flat fracture surface (Fig. 5A), while some small spheres (surrounded by red circle) appeared on the fracture surface of NMH3 which cross-linked by AAS nanospheres (Fig. 5B). More important, the size of the small spheres in NMH3 is similar to its original magnitude. This fact confirmed that AAS nanoparticles also maintain its nanoscale after the hydrogel formed. Therefore, the improvement in the mechanical properties of NMHs is presumably because of the even distribution of the cross-linking points in the hydrogel network. Because the flexible polymer chain length between the nanospheres is proportional to the interparticle distance, stress can be evenly distributed in the entire network, this makes crack initiation difficult. The effect of nanosphere concentration on the mechanical strength of NMHs is shown in Fig. 4B. Even small concentrations of nanoparticles incorporated in the hydrogel clearly improve its mechanical strength. Furthermore, the strain to failure decline as AAS nanospheres added because the cross-linking points become denser and the polymer chains between them become shorter. The fracture damage may occur when in a relatively smaller deformation. Although the strain to failure increase very little compare with that of CMH, the compressive strength significantly increases with increase in the nanosphere concentration, providing a convenient way to regulate the mechanical strength of NMHs.

### 3.5. Deswelling properties

Deswelling after a temperature jump from 5 °C (below the LCST, the hydrogels at equilibrated swollen state) to 30 °C (above the

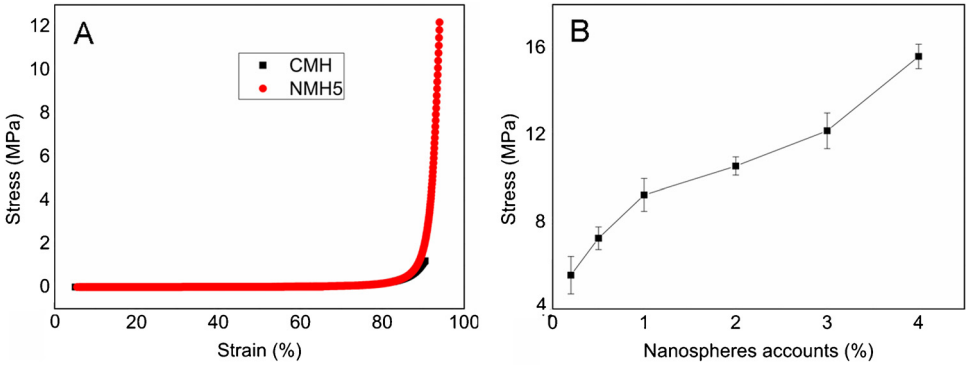


**Fig. 4.** Strain-stress curves for CMH and NMH5 (A) and the Effect of nanosphere concentration in NMHs on mechanical strength (B).

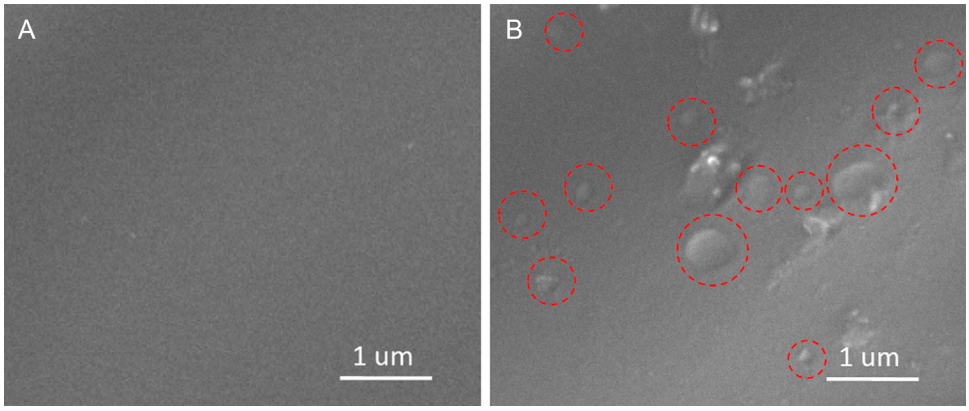


**Fig. 5.** SEM characterizations for fracture surface of freeze-dried CMH hydrogel (A) and NMH3 hydrogel (B).

LCST) in ultrapure water is presented in Fig. 6. Deswelling of NMHs is slightly faster than that of CMH, and all hydrogels reach deswelling equilibrium in 3 h. The characteristic time ($T$) for a hydrogel to shrink is given by Tanaka et al. (Tanaka, Sato, Hirokawa, Hirotsu, & Peetermans, 1985) and Ogawa et al. (Ogawa, Ogawa, & Kokufuta, 2004) as follows:

$$e^{(-t/T)} \sim \frac{Q_t - Q_e^c}{Q_e^s - Q_e^c} \quad (4)$$

where $Q_t$ represents the swelling ratio at time $t$; and $Q_e^s$ and $Q_e^c$ represent the equilibrium swelling ratios in the swollen and collapsed states, respectively.

The deswelling profiles of the CMH and NMHs show two stages: rapid shrinking on the minute time scale, followed by much slower water desorption. In the first stage ($\tau 1$), CMH, NMH3, and NMH5 hydrogels exhibit similar response characteristic times (4.5, 3.8, and 3.9 min, respectively). This transition can be attributed to a quick diffusion of water molecules into the surface of hydrogels. In the second stage ($\tau 2$), the response characteristic time of NMH5 hydrogel is 12.8 min, while that of CMH is 68.3 min. This faster response of NMHs results from the reduction of the osmotic pressure inside and outside of the skin layer by the homogeneous cross-linking networked structure of the hydrogel. It is noteworthy that $\tau 2$ of NMH3 is 24.3 min, indicating that the nanosphere concentration can efficiently regulate the rate of diffusion of water in the hydrogel network.

### 3.6. Degradation properties

The cross-linkers are biodegradable in the NMHs. We studied the hydrogel degradation using ATR-FTIR spectroscopy, monitoring the changes in the NMH5 hydrogel during the incubation in

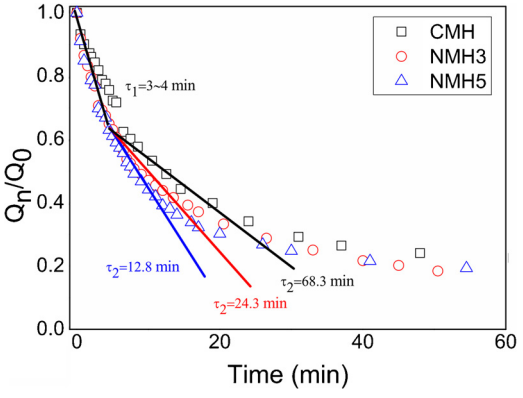


**Fig. 6.** Time course of deswelling of hydrogels undergoing shrinking in response to an abrupt temperature change from 5 to 30 °C.

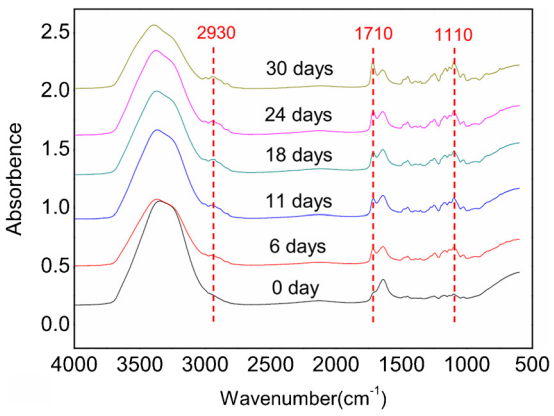


**Fig. 7.** Time course of degradation of NMH5 in 0.1 M PBS at pH 7.4.

phosphate buffered solution (PBS, pH 7.4) at 20 °C (below the LCST) for 0, 6, 11, 18, 24, and 30 d (Fig. 7). There was a clear increase in the intensity of the carboxylate C=O stretching band with time at ~1710 $cm^{-1}$. This increase most likely results from the degradation of the ester groups of $MEO_2MA$. In addition, the intensity of the characteristic peaks for methyl and methylene groups (~2830 to ~3000 $cm^{-1}$ and ~1100 to ~1200 $cm^{-1}$) also increased with time, presumably because of the degradation of AAS glucose units.

## 4. Conclusions

In this work, starch-based nanospheres are successfully used as cross-linkers for the fabrication of poly$MEO_2MA$ hydrogels. NMHs exhibit a narrow LCST range and high mechanical strength compared with conventional small molecule-cross-linked hydrogels. The swelling behavior of NMHs also differs from that of CMH. The hydrophilicity of starch-based nanospheres increases the equilibrium swelling rate. Moreover, the cross-linker nanospheres endow the hydrogel with a regular network structure, with the flexible polymer chain between the nanospheres being proportional to the interparticle distance. Therefore, NMHs show a sharper LCST gap, higher mechanical strength, and faster response rate than CMH. Therefore, the nanosphere concentrations efficiently regulate the various properties of NMHs. NMHs are also degradable in aqueous medium, as shown by FT-IR. Owning to its narrow LCST transition, high mechanical strength and degradable properties, the NMH hydrogels are very relevant for many application in material science such as intelligent thermal sensitive on-off, drug delivery, cell culture, etc. As nontoxicity and anti-immunogenicity, the NMH hydrogels can be used in biotechnology especially in the field of humanbody. In addition, the influence of degradation on the hydrogel mechanical strength and responsive properties, and in vitro and in vivo biosafety and bioavailability of the NMHs are still being investigated.

## Acknowledgement

Financial support from the National Natural Science Foundation of China (grant nos. 51103150 and 51321062) is gratefully acknowledged.

## References

Antonietti, M., Caruso, R. A., Göltner, C. G., & Weissenberger, M. C. (1999). Morphology variation of porous polymer gels by polymerization in lyotropic surfactant phases. *Macromolecules*, *32*, 1383–1389.

Bastide, J., & Leibler, L. (1988). Large-scale heterogeneities in randomly cross-linked networks. *Macromolecules*, *21*, 2647–2649.

Chang, C. W., Spreeuwel, van, Zhang, A., Varghese, C., & S. (2010). PEG/clay nanocomposite hydrogel: A mechanically robust tissue engineering scaffold. *Soft Matter*, *6*, 5157–5164.

Gao, X., Kucerka, N., Nieh, M. P., Katsaras, J., Zhu, S. P., Brash, J. L., & Sheardown, H. (2009). Chain conformation of a new class of PEG-based thermoresponsive polymer brushes grafted on silicon as determined by neutron reflectometry. *Langmuir*, *25*, 10271–10278.

Gates, B., Park, S. H., & Xia, Y. N. (2000). Tuning the photonic bandgap properties of crystalline arrays of polystyrene beads by annealing at elevated temperatures. *Advanced Materials*, *12*, 653–656.

Gotoh, T., Nakatani, Y., & Sakohara, S. (1998). Novel synthesis of thermosensitive porous hydrogels. *Journal of Applied Polymer Science*, *69*, 895–906.

Haraguchi, K., & Takehisa, T. (2002). Nanocomposite hydrogels: A unique organic–inorganic network structure with extraordinary mechanical, optical, and swelling/de-swelling properties. *Advanced Materials*, *14*, 1120–1124.

Haraguchi, K., Farnworth, R., Ohbayashi, A., & Takehisa, T. (2003). Compositional effects on mechanical properties of nanocomposite hydrogels composed of poly(*N*,*N*-dimethylacrylamide) and clay. *Macromolecules*, *36*, 5732–5741.

Hoshino, K., Taniguchi, M., Katagiri, M., & Fujii, M. (1992). Properties of amylase immobilized on a new reversibly soluble–insoluble polymer and its application to repeated hydrolysis of soluble starch. *Journal of chemical engineering of Japan*, *25*, 569–574.

Hu, Z. B., & Huang, G. (2003). A new route to crystalline hydrogels, guided by a phase diagram. *Angewandte Chemie International Edition*, *42*, 4799–4802.

Iizawa, T., Taketa, H., Maruta, M., Ishido, T., Gotoh, T., & Sakohara, S. (2007). Synthesis of porous poly(*N*-isopropylacrylamide) gel beads by sedimentation polymerization and their morphology. *Journal of Applied Polymer Science*, *104*, 842–850.

Iizawa, T., Yamamoto, D., Gotoh, T., & Sakohara, S. (2012). Synthesis of porous poly[oligo(ethylene glycol)methyl ether methacrylate] gels that exhibit thermosensitivity in highly concentrated aqueous NaCl solution. *Polymer*, *53*, 3417–3420.

Israelachvili, J. (1997). The different faces of poly(ethylene glycol). *Proceedings of National Academy of Sciences of the United States of America*, *94*, 8378–8379.

Juliano, B. O., Perez, C. M., Blakeney, A. B., Castillo, T., Kongseree, N., Laignilet, B., Lapis, E. T., Murty, V. V. S., Paule, C. M., & Webb, B. D. (1981). International cooperative testing on the amylose content of milled rice. *Starch*, *33*, 157–162.

Kwon, I. C., Bae, Y. H., & Kim, S. W. (1991). Electrically erodible polymer gel for controlled release of drugs. *Nature*, *354*, 291–293.

Lee, Y. J., & Braun, P. V. (2003). Tunable inverse opal hydrogel pH sensors. *Advanced Materials*, *15*, 563–566.

Liu, K. H., Liu, T. Y., Chen, S. Y., & Liu, D. M. (2008). Drug release behavior of chitosan–montmorillonite nanocomposite hydrogels following electrostimulation. *Acta Biomaterialia*, *4*, 1038–1045.

Luo, Y., Kirker, K. R., & Prestwich, G. D. (2000). Cross-linked hyaluronic acid hydrogel films: New biomaterials for drug delivery. *Journal of Controlled Release*, *69*, 169–184.

Lutz, J. F., Akdemir, O., & Hoth, A. J. (2006). Point by point comparison of two thermosensitive polymers exhibiting a similar LCST: Is the age of poly(NIPAM) over? *Journal of the American Chemical Society*, *128*, 13046–13047.

Lutz, J. F., Andrieu, J. S., Üzgün, S., Rudolph, C., & Agarwal, S. (2007). Biocompatible, thermoresponsive, and biodegradable: Simple preparation of "all-in-one" biorelevant polymers. *Macromolecules*, *40*, 8540–8543.

Lutz, J. F., & Hoth, A. (2006). Preparation of ideal PEG analogues with a tunable thermosensitivity by controlled radical copolymerization of 2-(2-methoxyethoxy)ethyl methacrylate and oligo(ethylene glycol)methacrylate. *Macromolecules*, *39*, 893–896.

Lutz, J. F., Weichenhan, K., Akdemir, O., & Hoth, A. (2007). About the phase transitions in aqueous solutions of thermoresponsive copolymers and hydrogels based on 2-(2-methoxyethoxy)ethyl methacrylate and oligo(ethylene glycol)methacrylate. *Macromolecules*, *40*, 2503–2508.

Maeda, Y., Kubota, T., Yamauchi, H., Nakaji, T., & Kitano, H. (2007). Hydration changes of poly(2-(2-methoxyethoxy)ethyl methacrylate during thermosensitive phase separation in water. *Langmuir*, *23*, 11259–11265.

Matsubara, K., Watanabe, M., & Takeoka, Y. (2007). A thermally adjustable multicolor photochromic hydrogel. *Angewandte Chemie International Edition*, *46*, 1688–1692.

Narumi, A., Otsuka, I., Matsuda, T., Miura, Y., Satoh, T., Kaneko, N., Kaga, H., & Kakuchi, T. (2006). Glycoconjugated polymer: Synthesis and characterization of poly(vinyl saccharide)-block-polystyrene-block-poly(vinyl saccharide) as an amphiphilic ABA triblock copolymer. *Journal of Polymer Science Part A: Polymer Chemistry*, *44*, 3978–3985.

Ogawa, Y., Ogawa, K., & Kokufuta, E. (2004). Swelling–shrinking behavior of a polyampholyte gel composed of positively charged networks with immobilized polyanions. *Langmuir*, *20*, 2546–2552.

Serizawa, T., Wakita, K., & Akashi, M. (2002). Rapid deswelling of porous poly(*N*-isopropylacrylamide) hydrogels prepared by incorporation of silica particles. *Macromolecules*, *35*, 10–12.

Sharma, A. C., Jana, T., Kesavamoorthy, R., Shi, L. J., Virji, M. A., Finegold, D. N., & Asher, S. A. (2004). A general photonic crystal sensing motif: Creatinine in bodily fluids. *Journal of the American Chemical Society*, *126*, 2971–2977.

Shibayama, M. (1998). Spatial inhomogeneity and dynamic fluctuations of polymer gels. *Macromolecular Chemistry and Physics*, *199*, 1–30.

Tan, Y., Wang, P. X., Xu, K., Li, W. B., An, H. Y., Li, L. L., Liu, C., & Dong, L. S. (2009). Designing starch-based nanospheres to make hydrogels with high mechanical strength. *Macromolecular Materials and Engineering*, *294*, 855–859.

Tan, Y., Xu, K., Wang, P. X., Li, W. B., Sun, S. M., & Dong, L. S. (2010). High mechanical strength and rapid response rate of poly(*N*-isopropyl acrylamide) hydrogel cross-linked by starch-based nanospheres. *Soft Matter*, *6*, 1467–1471.

Tanaka, T., Sato, E., Hirokawa, Y., Hirotsu, S., & Peetermans, J. (1985). Critical kinetics of volume phase transition of gels. *Physical Review Letters*, *55*, 2455–2458.

Tasaki, K. (1996). Poly(oxyethylene)-water interactions: A molecular dynamics study. *Journal of the American Chemical Society*, *118*, 8459–8469.

Xu, K., Tan, Y., Chen, Q., An, H. Y., Li, W. B., Dong, L. S., & Wang, P. X. (2010). A novel multi-responsive polyampholyte composite hydrogel with excellent mechanical strength and rapid shrinking rate. *Journal of Colloid and Interface Science*, *345*, 360–368.

Zhang, X. Z., & Zhuo, R. X. (2001). Dynamic properties of temperature-sensitive poly(*N*-isopropylacrylamide) gel cross-linked through siloxane linkage. *Langmuir*, *17*, 12–16.